A REVIEW OF LOW ENERGY SPUTTERING THEORY AND EXPERIMENTS

Olivier B. DUCHEMIN*
California Institute of Technology, Pasadena, CA 91125

John R. BROPHY† and Charles E. GARNER‡
Jet Propulsion Laboratory, Pasadena, CA 91109

Pradosh K. RAY§ and V. SHUTTHANANDAN¶
Tuskegee University, Tuskegee, AL 36088

Maris A. MANTENIEKS#
Lewis Research Center, Cleveland, OH 44135

Abstract

Sputtering mechanisms relevant to the erosion processes of electron bombardment xenon ion engines are described. Practical semi-empirical formulations applicable for slow, heavy ions are reviewed, along with the existing data for the sputtering of molybdenum by very low-energy xenon ions. No experimental data are available under 100 eV. Finally, seven different types of experimental techniques for measuring low-energy sputtering are reviewed.

1. Introduction

On-going efforts to assess xenon ion engine service life are hindered by the lack of qualitative and quantitative knowledge of the physical phenomena governing ion engine failure modes. Brophy *et al.*[1] identified seven distinct failure modes for the NSTAR (NASA Solar Electric Propulsion Technology Application Readiness) engine.

Two of these failure modes involve direct impact of unfocused primary xenon ions on the molybdenum screen grid webbing. One mode corresponds to structural failure of the screen grid, while the other is caused by structural failure of the accelerator grid due to direct ion impingement from beamlets defocused by flakes of sputtered material on the screen grid. The screen grid itself is believed to be the primary source of sputtered material.[1] Another of these failure modes results from cathode orifice plate erosion, due to sputtering by ions with kinetic energies having a DC component between 12 and 20 eV for NSTAR.

In the two cases involving screen grid erosion, the kinetic energy of the incident ions corresponds to the engine discharge voltage. Despite successive reductions of discharge voltage values over the past years to the present value of less than 25 V for NSTAR in an effort to reduce the sputter erosion rates, the impingement of these low-energy ions is still believed to potentially lead to structural failure of the screen grid or the production of sputter deposited films which in turn can form metallic flakes that migrate in the chamber and can interfere with the optics. This erosion process, in the presence of a significant amount of double ions, can compete with the higher-energy sputtering erosion of the accelerator grid by charge-exchange ions because of a much higher incident ion current density.

However, the extremely long duration of life demonstration tests (8000-12000 hr.) and their cost make it impractical to rely on testing alone to predict ion engine service life. In addition, the level of confidence one has in the interpretation of tests involving different engine designs or different operating modes is dependent upon the understanding of the physical processes involved.[1] For instance, knowledge of the low-energy sputtering yield for the incident ions on the screen grid material is necessary in order to analyze and predict the occurrence of screen grid failure or flake formation.

A great amount of research over the last five decades has been motivated by interest in subjects such as surface cleaning, sputter deposition of thin films or etching by sputtering, and has been carried out on high-energy (greater than a few keV) sputtering yields. In particular, the sputtering mechanism for light ions received attention from attempts at understanding the erosion of planetary surfaces by the solar wind[2,3] or investigations of the magnetic confinement of hydrogen plasmas for fusion reactors.[4] However, little is known about very low-energy sputtering by heavy ions. This lack of data results in the use of extrapolations from high-energy measurements or semi-empirical formulae that are inherently uncertain to generate estimates for the wear-out rate.

* Graduate Student, Aeronautical Engineering
† Group Supervisor, Advanced Propulsion Technology Group
‡ Senior Engineer, Advanced Propulsion Technology Group
§ Professor, Mechanical Engineering
¶ Research Assistant Professor, Mechanical Engineering
# Aerospace Engineer

In this paper we present an overview of the physical description of low-energy sputtering and measurement techniques or results. We also describe the different methods available for generating approximate values.

2. Low Energy Sputtering: A Description

The interaction between an incident particle and a solid target can give rise to many different phenomena: the particle can be backscattered, come to thermal equilibrium with the surface before being subsequently evaporated, excite electronic transitions and provoke the ejection of gamma (secondary) electrons or the modification of chemical bonds, dislodge atoms from the solid surface or even, at very high particle energies, cause radiation damage.[5] The kinetic energy of the incoming particle determines, for the most part, which phenomenon actually occurs or dominates.

Physical sputtering is an atomic scale process[6] that can occur if the incident particle (ion) can transfer sufficient energy to a surface or bulk target atom to overcome its bulk displacement energy and/or its surface binding energy. The erosion due to physical sputtering is described by the sputtering yield, Y, a statistical variable defined as the mean number of atoms removed from a solid target per incident ion. Sputtering by elastic collisions can have three regimes: the single-knockon, the linear cascade or the spike regime.[6]

The processes involving a linear collision cascade or the spike regime become less important at energies near threshold. Behrisch[7] summarized the possible sputtering mechanisms for low-energy light ions as reproduced in Fig. 1. These mechanisms are in fact still possible for heavy ions on light targets, as is most often the case with xenon, with the provision that the processes involving an outgoing ion (S_{II}) are less probable than with light ions since backscattering of a heavy ion (impossible for a head-

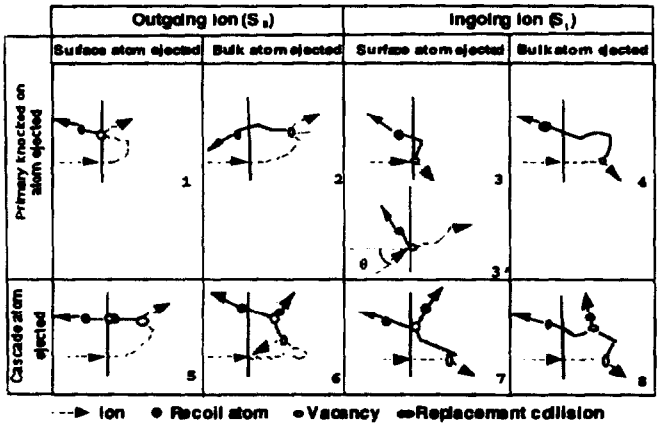

Fig. 1: A "billiard-ball" description of possible sputtering mechanisms.[7]

on collision) will demand more collisions. In the case of normal ion incidence, a minimum of two collisions are necessary for producing a sputtered atom. In turn, atoms sputtered as a result of very few low-energy collisions are more likely to be sputtered at grazing incidences.[8,9]

A pure hard-sphere, classical two-particle elastic scattering model is often used to describe physical sputtering, but the energy transfer between ions and atoms or between two cascade atoms is complicated by the complex electronic screening of the two nuclei.[10] In the limit of high-energy particles, the collision kinematics are the same as in Rutherford scattering of two point charges, but for low-energy collisions a detailed description would require taking into account the physics of quantized screened Coulomb collisions and the absorption of energy by Pauli promotion of the electrons.[10] Finally, the nuclear stopping power, i.e., the probable energy loss of the ion per unit distance traveled through the target, depends on which classical atomic model is chosen.[10] Unfortunately, these models give significantly different results at low energy, as shown on the plot reproduced for convenience in Fig. 2.

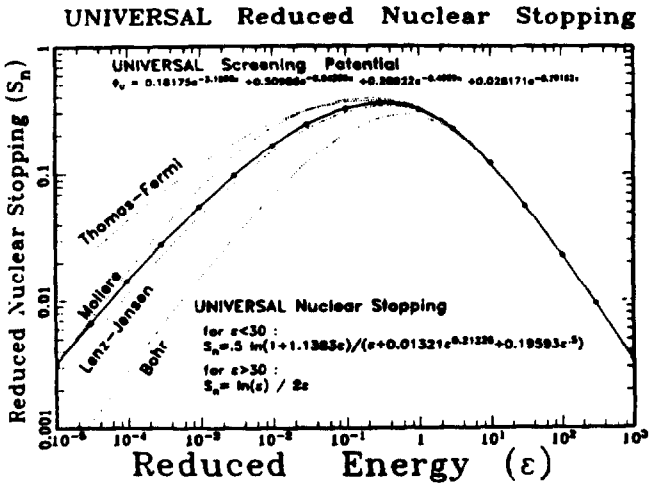

Fig. 2: Nuclear stopping power using the universal screening potential (solid line) or the four classical atomic models.[10]

It should also be noted that at energies near threshold a new difficulty arises, due to the fact that the Rutherford scattering cross section increases with decreasing particle velocity. This in turn implies that the collisions can no longer be treated as independent binary collisions, but rather involve several neighboring atoms.[5,11,12]

Threshold Energy And Atomic Mass Dependence

Since physical sputtering is a collision process, it is intuitive that it should be a function of the atomic mass of the collision partners. It can easily be shown (see e.g. Ref. 10) that the fraction of energy transferred to a target particle of mass m_2 by a projectile of mass m_1 in a head-on (zero scattering angle) collision is:

$$\gamma \equiv \frac{E_2}{E_0} = \frac{4m_1m_2}{(m_1+m_2)^2} \qquad (1)$$

where γ is the energy transfer factor, E_2 is the kinetic energy transferred to the target particle and E_0 is the initial kinetic energy of the projectile.

Bradley[13] concluded from this and early experiments in 1954 that the threshold (or minimum)

energy for sputtering to occur could be predicted by:

$$\frac{U_S}{E_{th}} = \frac{4m_1m_2}{(m_1+m_2)^2} = \gamma \qquad (2)$$

where U_S is the atomic heat of sublimation and E_{th} the threshold energy. This was later confirmed by Wehner[12] who, in 1958, suggested that in a first approximation E_{th} was proportional to U_S/γ, with the proportionality factor being between 8 and 20. He also noted that sputtering presented quite the same periodicity with atomic number as the heat of sublimation.

However a somewhat counterintuitive result was published in 1962 by Stuart and Wehner,[14] who first realized that in fact the mass ratio between ion and target atom played hardly any role in the thresholds. This observation was then confirmed by Wehner and Anderson[5] who suggested as an explanation that at low energy the collisions could not be treated as independent successive two-particle collisions and recommended that "modified masses" be introduced. The fractional energy transfer γ was therefore dropped from some models used to predict the sputtering threshold, but the value of E_{th} was still controversial and subsequently approximated as $4U_S$ for heavy ions[4] or both for heavy and light ions,[5] U_S/γ for light ions[15,16] or for $m_1<<m_2$,[17] $U_S/\gamma(1-\gamma)$ for $m_1/m_2 \le 0.3$,[17] $8U_S(m_1/m_2)^{2/5}$ for $m_1/m_2>0.3$,[17]

$$E_{th} = 1.5\frac{U_s}{\gamma}\left[1+1.38\left(\frac{m_1}{m_2}\right)^h\right]^2 \qquad (3)$$

where h=0.834 for $m_2>m_1$ and h=0.18 for $m_2<m_1$,[18] or finally

$$E_{th} = U_s\left[1.9+3.8\left(\frac{m_2}{m_1}\right)^{-1}+0.134\left(\frac{m_2}{m_1}\right)^{1.24}\right] \qquad (4)$$

where Eq. (4) is from Ref. 19. For completeness, it should be added that Weissman and Sigmund[11] suggested $E_{th} \approx U_s$ and Olson *et al.*[9] pointed out that the very poorly defined sputtering threshold (identified as the surface binding energy) may have an effective value much less than the heat of sublimation. Which approximation is to be used, except for Eq. (4), depends on which sputtering mechanism dominates (see Fig. 1). As pointed out by Weissmann and Behrisch,[20] sputtering by light ions is primarily driven by backscattering of the ions from the interior of the target (reflective collision process), whereas for heavy ions collision cascades generated by direct impingement of the incoming ions dominate the sputtering mechanism (displacement process). This distinction is extremely important for the threshold energy, as well as for the angular dependence of the low-energy sputtering yield.[21]

Incidence Angle Dependence

Ref. 21 provides an excellent background as well as an extensive list of references on the subject of angular dependence of sputtering yields that will not be duplicated here. Yamamura *et al.*[21] reported that numerous investigations showed the angular dependence of the sputtering yield to behave like $\cos^{-f}\theta$ for not-too-oblique incidence, where θ is the angle of incidence measured from the surface normal, while Sigmund[22] obtained from theoretical studies a dependence in $\cos^{-f}\theta$, where $1<f<2$. Yamamura *et al.*[19] pointed out that the threshold energy for heavy-ion sputtering was mainly determined by the anisotropic velocity distribution of the recoil atoms, and Yamamura *et al*[21] further indicated that this was also the reason why the threshold energy had a minimum near 60°, unlike in the case of light-ion sputtering.

An empirical formula for the angular dependence of sputtering can be given as:[21]

$$\frac{Y(\theta)}{Y(0)} = \cos^{-f}\theta \exp\left[-\Sigma\left(\cos^{-1}\theta - 1\right)\right] \qquad (5)$$

where f and Σ are energy-dependent fit parameters as given in Ref. 21, with values 19.96 and 13.55 respectively for 100-eV xenon ions on molybdenum. $Y(0)$ is the sputtering yield at normal incidence. The exponent f carries the threshold effect and is a function of the ratio E/E_{th}. The angular dependence of E_{th} itself is driven by the the threshold energy for the sputtering process S_1 in Fig. 1 and the threshold energy corresponding to surface channeling,[21] i.e.

$$E_{th}(\theta) \equiv E_{th}(0)\cos^2\theta \qquad (6a)$$

for not-too-oblique incidence angles, and

$$E_{th}(\theta) \equiv \frac{0.3\dfrac{m_1/m_2}{m_1/m_2+1}E_{TF}\left(\dfrac{a}{R_o}\right)^3}{\cos^2\theta} \qquad (6b)$$

for grazing angles. $E_{th}(0)$ is the threshold energy for normally-incident ions, a is the Thomas-Fermi screening radius and is a function of the atomic numbers Z_1 and Z_2 of the projectile and the target respectively and is given by

$$a = 0.4685\left(Z_1^{2/3}+Z_2^{2/3}\right)^{-1/2}, \qquad (7)$$

R_0 is the average lattice constant of the target, given by $R_0 = N^{-1/3}$ where N is the number density of the target atom, and E_{TF} is the Thomas-Fermi energy unit given by

$$E_{TF} = \frac{m_1+m_2}{m_2}\frac{Z_1Z_2e^2}{a} \qquad (8)$$

from LSS theory (see for example Refs. 6, 10 or 23). e is the proton charge. Eq. (6a) corresponds to the sputtering mechanism S_1 (see Fig. 1), while Eq. (6b) describes the onset of surface channeling and dominates for large values of θ. Fig. 3 shows the threshold energy as a function of incidence angle for these two mechanisms for xenon ions on molybdenum. The angular dependence of the sputtering yield for 100-eV xenon ions on molybdenum using Eq. (5) is also shown.

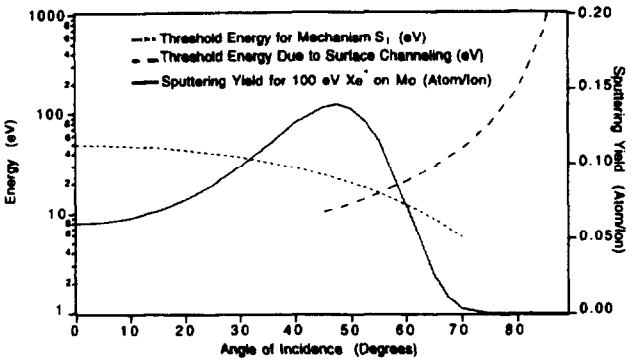

Fig. 3: Angular dependence of the threshold energy and sputtering yield for 100 eV-Xe$^+$ ions on Mo. The sputtering mechanism S_t dominates for heavy ions at not-too-oblique angles, while the threshold energy corresponding to surface channeling applies for grazing angles of incidence[21].

3. Predictions for Low-Energy Sputtering

Empirical Formulae

In order to predict the ion erosion rate on the NSTAR engine, Rawlin[24] used a quadratic approximation to extrapolate the energy dependence of the sputtering yield in the region near threshold. Other authors have developed or used empirical or semi-empirical models.

Sigmund[22] proposed a systematic study of the sputtering of a random monoatomic target in the linear collision cascade regime based on transport theory. The Sigmund equation,

$$Y(E) = \frac{0.042\,\alpha(M_2/M_1)S_n(E)}{U_s} \qquad (9)$$

gives the energy dependence of the yield $Y(E)$ as a function of the measured sublimation energy U_s, the elastic (nuclear) stopping cross section $S_n(E)$, and the fit parameter $\alpha(M_2/M_1)$. Matsunami *et al.*[25] adapted this formula by taking into account the effect of the threshold energy to write the first Matsunami formula:

$$Y(E) = \frac{0.42\,\alpha K s_n(\varepsilon)}{U_s}\left[1-\left(\frac{E_{th}}{E}\right)^{1/2}\right] \qquad (10)$$

where $\varepsilon = E/E_{TF}$ is the reduced energy, $s_n(\varepsilon)$ is Lindhard's elastic reduced stopping cross section and K is the conversion factor from $s_n(\varepsilon)$ to $S_n(E)$, as defined in Ref. 25. Yamamura *et al.*[26] further refined this equation by making the inelastic stopping explicit in:

$$Y(E) = \frac{0.042\,\alpha S_n(E)}{U_s\left[1+0.35U_s s_e(\varepsilon)\right]}\left[1-\left(\frac{E_{th}}{E}\right)^{1/2}\right]^2 \qquad (11)$$

where $S_e(\varepsilon)$ is Lindhard's reduced inelastic (electronic) stopping cross section. Finally, Yamamura *et al.*[27] rewrote Eq. (11) to take into account the effect of the target material on the mass-ratio dependence, i.e. by substituting $\alpha(M_2/M_1)$ by $Q(Z_2)\alpha^*(M_2/M_1)$ to yield the third Matsunami formula:

$$Y(E) = \frac{0.042\,Q\alpha^* S_n(E)}{U_s\left[1+0.35U_s s_e(\varepsilon)\right]}\left[1-\left(\frac{E_{th}}{E}\right)^{1/2}\right]^{2.8} \qquad (12)$$

Appropriate tables and definitions to obtain the numerical values of the different parameters for 259 ion-target combinations are given in Ref. 28. E_{th} is given by Eq. (4).

Similarly, Bohdansky developed both a formulation valid only for light ions[17] and the universal relation below:[29]

$$Y(E) = \frac{0.042\,\alpha S_n(E)}{U_s}\left(\frac{R_p}{R}\right)\left[1-\left(\frac{E_{th}}{E}\right)^{2/3}\right]\left[1-\left(\frac{E_{th}}{E}\right)\right]^2 \qquad (13)$$

where E_{th} takes the value $8U_s(m_1/m_2)^{2/5}$ and R_p/R is given by:

$$\frac{R}{R_p} = 0.4\,M_2/M_1 + 1 \qquad (14)$$

if inelastic losses are neglected.[29]

A plot showing the energy dependence of the sputtering yield of molybdenum with xenon ions using the formulation given by the third Matsunami formula and Eq. (13) is shown in Fig. 4. Results of computer calculations with the Monte-Carlo simulation code TRIM and experimental data are also shown.

The third Matsunami formula or Eq. (13), along with Eq. (5), are helpful analytical expressions, and were used by Bond and Latham[30] in the plasma simulation code SAPPHIRE to calculate grid erosion rates due to charge-exchange ions in the UK-10 ion thruster. Sigmund[22]

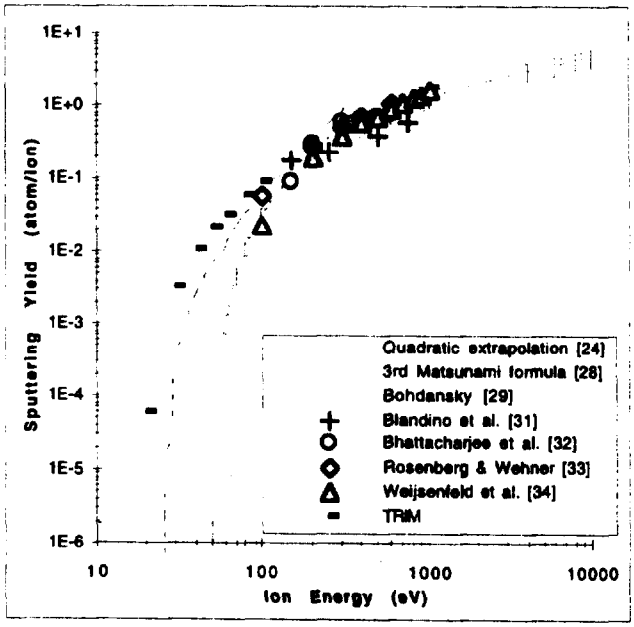

Fig. 4: Energy dependence of the sputtering yield of molybdenum with xenon ions. The 3rd Matsunami formula is plotted with error bars corresponding to a 28.6% uncertainty on the parameter Q.[28]

however noted in his theory that the surface collisions that dominate sputtering near threshold cannot be described by transport theory, and that the concept of binary collisions that he assumed becomes questionable at low energy.

Extreme care should therefore be used with Eqs. (9)-(12) at energies near threshold.

4. *A Review of Experimental Methods*

Driving Requirements

Measuring sputtering yields for materials of interest in ion thruster technology with slow incident ions raises very serious experimental difficulties,[14,35] listed below:

- The vanishingly small amounts of sputtered material to be measured in a practical exposure time mandates the use of an extremely sensitive method and requires as high an ion current density as possible.

- The ion beam should have as low an energy spread and as low a divergence angle as possible, to insure that the ion energy and incidence angle are well known and controlled. This implies in particular that the multiply-charged ion current be as small as possible, which requires a low discharge voltage. Another concern regarding the beam could be the presence of fast neutrals due to charge exchange collisions in the ion source. The choice for the method of generating the ion beam usually results from a trade off between the relatively high current densities achievable with a plasma discharge (typically up to 15 mA/cm^2) and the better-defined beam that can be obtained with an ion gun, in terms of energy, incidence angle and impurities. Ion guns however are limited in beam current density due to the space charge limitation, proportional to $V^{3/2}$ where V is the accelerating voltage.

- A low background gas pressure needs to be achieved in the facility in order to insure that the mean free path of the ions is larger than the source-to-target distance, so that uniformity of the beam in energy and incidence angle is preserved. A low base pressure is also required to prevent the formation of a protective chemisorbed impurity layer at the target surface. This problem is also related to the ion beam current density and is described in more detail below.

Effects of Background Gases on Sputter Erosion in Ion Thrusters

Lifetests of ion thrusters to measure the screen grid sputter-erosion may be seriously compromised by the effects of background gases.[36,37] Erosion by unfocused ions in the discharge chamber is lowered in the presence of background gases. The sputtering rate of the screen grid has been found to be reduced from that of a dynamically clean surface by factors up to eight. If vacuum conditions are not adequate in the test facility, the various species of background gases will be chemisorbed on the screen grid surface and will act as a buffer to the impinging ions, thus reducing the net erosion rate of the screen grid. This effect is shown in Fig. 5. The plasma in the discharge chamber excites the background gas molecules, which dissociate upon colliding with the target surface. This increases the reactivity of the background gases. When the pressure is sufficiently low, the sputter-erosion rate is equal to that of a dynamically clean surface. As the background pressure is increased, chemisorption on the screen grid surface will begin to take place. If the background pressure reaches still higher levels, the sputter-erosion will level off as compound or compounds of the target and the background gases[38] are formed. Under these conditions, the sputtering of the compound or compounds will take place instead of a clean surface. The pressure at which chemisorption will begin to affect the measured sputtering rate depends on the thruster operating condition, the discharge voltage which determines the ion energy, and the current density of the singly and doubly charged ions.

To determine the proper vacuum conditions at which the effect of the background gases becomes negligible for the operating conditions of the thruster is no easy task. It has often been stated that a sufficient condition for a dynamically clean surface is that the flux of the impinging ions be larger than the flux of the impinging gas to the target area.[39] This, however, is not a sufficient condition. The sputtering rate of the absorbed species has to be taken into account. The condition to ensure a dynamically clean surface is:[6]

$$\frac{Y_{i,s} I}{f \beta_{i,s}} \geq 10 \qquad (15)$$

where: $Y_{i,s}$ = sputtering yield of species i absorbed on target s
I = ion flux impinging on target s
f = background gas flux impinging on target s
$\beta_{i,s}$ = sticking probability of background gas species i on a clean target s

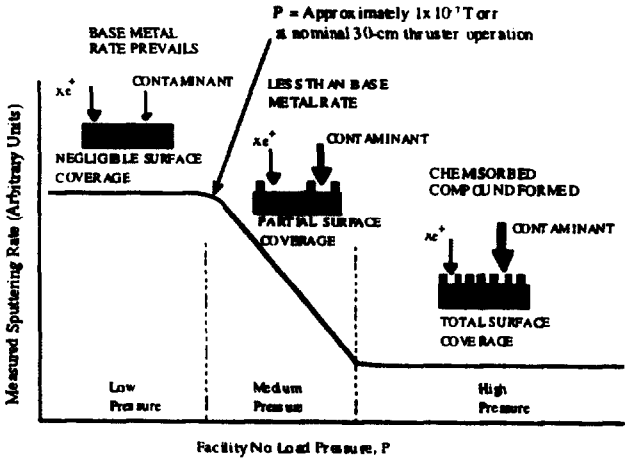

Fig. 5: Sputtering rate as a function of facility no load pressure.

The parameters most difficult to determine are $Y_{i,s}$ and $b_{i,s}$. A theory for the sputtering of chemisorbed gases has been developed[40,41] and the formulations applied to thruster lifetime tests met with some degree of success.[37] It has been demonstrated that most background gases found in diffusion pump vacuum facility such as N_2, H_2O, O_2 and

C_2N_2, will react with the target and be chemisorbed on the target.[42]

To calculate the ratio defined by Eq. (15), it is assumed that the bulk of the chemisorbed gas on the screen grid target is nitrogen. In a common diffusion pump vacuum facility in which an air leak or liquid nitrogen trap leak is the most probable source of background gas, nitrogen is the largest constituent of the background gases. The sputtering yields of chemisorbed nitrogen were calculated using Winter's formulation.[41] For NSTAR conditions, the sputter yield of nitrogen for singly charged xenon ions at 25 V is 0.02 atom/ion and for doubly charged xenon ions, the yield is 0.08 atom/ion. The sticking coefficient was assumed to be equal to 1.0 because of the high reactivity of the species due to the presence of the discharge plasma. The ratio defined by Eq. (15) is estimated to be 5 for the given test conditions, which is somewhat lower than the recommended value of 10. Therefore, some reduction of the sputtering rate of the screen grid is to be expected in a lifetest due to background gases, if the operating pressure of the vacuum facility is ~2.0 x 10^{-7} Torr. The magnitude of the reduction is not well defined.

Measurement Techniques and Results

A brief review of experimental techniques follows, and is summarized in Table 1. Seven families of methods for measuring sputter yields have been identified. Other early methods from the 1920's through 1950's, some of which were reasonably sensitive, are not listed here but are described in Ref. 14.

The first and most extensively used method involves measuring the weight loss of the eroded sample.[12,16,33-35,43-46] While this method allows for absolute, direct measurements on all materials and is relatively simple, its sensitivity, limited to about 10^{-3} atom/ion with

Method	Comments	Ref.	Ion/Target Combination	Ion Beam Generation	Ion Energy Range (eV)	Beam Current Density (mA/cm^2)	Background Pressure (Torr)	Lowest Sputtering Yield Measured (atom/ion)
Weight Loss	-Direct, versatile, absolute values -Low sensitivity	33	Hg^+ on 26 metals	Plasma disch.	30-400	~5 (up to 15)	~ 10^{-6}	~$1x10^{-2}$
		12	Hg^+ on metals and semiconductors	Plasma disch.	50-400	~5 (up to 15)	~ 10^{-6}	~0.2
		41	Ar^+ and Ne^+ on metals and semiconductors	Plasma disch.	50-600	2-15	~$7x10^{-7}$	$4x10^{-3}$
		31	Ni^+, Ar^+, Kr^+ and Xe^+ on Cu, Ni, Fe and Mo	Plasma disch.	100-1000	~1.5	-	~0.1
		30	He+, Kr+, and Xe+ on various metals	Plasma disch.	100-600	2-15	10^{-6}-10^{-7}	$1x10^{-3}$
		42	H_2^+ on 304 SS, pyro. graphite, C fibres, glassy C and SiC	Ion source	500-7,500	Up to 5	-	$3x10^{-3}$
		16	H^+, D^+, $^3He^+$ and $^4He^+$ on Mo and Au	Ion Source	150-20,000	0.5 to 1	~10^{-7}	$1x10^{-4}$
		43	Selfsputtering for Ni	Plasma disch.	75-3,000	0.1	-	$7x10^{-2}$
		44	H^+ and He^+ on Ni and W	Ion source	1,000-4,000	0.5 to 5	~10^{-7}	$2.1x10^{-3}$
Profilometry	-Direct, versatile, absolute values -Low sensitivity	47	Ar^+ on Si, Ag, Cu, Ni, Ti and Al	Ion gun	10,000	0.1	-	~10^{-2} (inferred)
		31, 48	Xe^+ on CVD diamond, C-C and Mo	Ion source	150-750	0.3-2.6	~10^{-9}	0.1
Optical. Transmission	-Versatile, *In situ* -Relative values, indirect	49	Hg^+ on metals	Compressed plasma disch.	20-200	Up to 500	-	$3x10^{-4}$
Surface Ionization	-Sensitive, direct -Limited to alkali metals, relative values	13	He^+, Ne^+, Ar^+ and Xe^+ on Na and K	Ion gun	0-1,800	-	$5x10^{-8}$	$3x10^{-3}$
Radioactive Tracer	-Very sensitive, direct -Few suitable isotopes, relative values, complex	50	Hg^+ and Ar^+ on Co	Plasma disch.	10-100	-	-	$1x10^{-4}$
		51	Ar+ and Xe+ on Co, Cd and Cr	Ion gun	10-500	Up to 0.1	$2x10^{-7}$	$2x10^{-5}$
		52	Ar^+ and Xe^+ on Cr	Ion gun	50-500	0.01-0.1	$2x10^{-7}$	$5x10^{-2}$
		53	Ar^+ and Xe^+ on Co and Cr	Ion gun	10-50	0.002-0.02	$2x10^{-7}$	$4x10^{-5}$
QCM	-Very sensitive, absolute, simple, direct, *in situ* -Requires sample material to be coated as thin film on crystal	55	Ar^+ on Au	Ion source	0-100	~0.01	$1x10^{-7}$	$3x10^{-3}$
		56	Selfsputtering for Au, Cu, Ag, Cr and Al	Ion gun	10-500	-	$2x10^{-7}$	~10^{-3} (1.1 in less than 10 sec.)
Spectroscopic Methods	-Very sensitive, versatile, *in situ* -Often indirect and giving relative values	57	Hg^+ and Ar^+ on Cr	Plasma disch.	25-300	-	-	10^{-4}
		14	Ne^+, Ar^+, Kr^+, Xe^+ and Hg^+ on 23 metals	Compressed plasma disch.		40 (up to 100)	$1x10^{-6}$	10^{-3}
		59	Ar^+ on Ag and Nb	Ion source	500-1,500	0.08 (estimate)	$1.5x10^{-9}$ w/o bakeout	0.2 measured 10^{-3} possible
		32	Xe^+ on Mo	Ion gun	150-600	0.03	$2x10^{-9}$	0.1

Table 1: A Review of Experimental Techniques for Measuring Low Sputtering Yields.

very high beam current densities, makes it inappropriate for sputtering at energies near threshold.

The same remarks apply to profilometry.[31,47,48] This method involves measuring the depth of the sputtered surface with a micro-stylus, with reference to a masked area of the target. One difficulty with this method is that its precision depends on the eroded depth profile roughness.

Askerov and Sena[49] used the change in the optical transmission of the plasma radiation to a photoresistor through the sputtered film deposited on a glass wall. Although this method has the advantage of being *in situ*, it is indirect, gives a relative value for the sputtering yield and is still of too low a sensitivity for very slow ions.

Another somewhat original and relatively sensitive method was described by Bradley,[13] who used the property that alkali metal atoms lose their valence electron when striking a hot metal surface. In these experiments, a negatively-biased electrode collected the ion current corresponding to the sputtered alkali atoms ionized upon impact on a hot platinum surface. This method is unfortunately confined to alkali metals and only gives relative sputtering coefficients.

Methods using radioactive tracers were proved by Morgulis and Tishchenko[50] and Handoo and Ray[51-53] to provide a great benefit in sensitivity, enabling measurements in the near threshold region. These methods however presents the inconvenience of requiring a suitable isotope for the material to be sputtered (in terms of half life and energy of the gamma-ray emissions) or the activation of a surface layer of the sample in a specialized facility.[54]

Another very sensitive method, using Quartz Crystal Microbalance (QCM) techniques, was early proposed by McKeown.[55] With modern-day frequency-measurement technology, using a QCM could theoretically enable direct, *in situ*, measurements of sputter yields as low as 10^{-5} atom/ion even at low current density. A difficulty associated with this method is that it requires the sample material to be coated as a thin film (a few μm thick) on the quartz crystal.

The last family of measurement techniques encompasses spectroscopic methods such as optical spectroscopy,[14,57,58] Auger Electron Spectroscopy (AES),[59] Rutherford Backscattering Spectroscopy (RBS),[32] or Secondary Neutral Mass Spectrometry (SNMS).[32] Optical spectroscopy and SNMS are indirect methods and can only give relative sputtering yields. RBS was used by Bhattacharjee *et al.*[32] to calibrate measurements obtained with SNMS, which are more sensitive.

5. Current Work and Conclusion

Upon reviewing the literature available on low energy sputtering yields, the authors have concluded that:

(a) There is currently no satisfactory data available for the sputtering yield of molybdenum by xenon ions under 100 eV to adequately assess ion engine service life by analysis.

(b) Extrapolations and semi-empirical formulae are available to obtain rough estimates with an uncertainty exceeding 20%.[28] They are based on fit parameters obtained with existing, higher-energy data.

(c) Empirical formulations or computer simulations are based on physical theories that break down at low energy because the interatomic potentials and the assumptions on the nature of the collisions no longer represent an accurate description of the reality.

(d) The measurement of sputtering yields with energies near threshold poses serious difficulties, essentially due to contamination issues and sensitivity requirements.

However, modern instruments, measurement techniques and vacuum facilities might enable some significant progress in the near future. Experimental work is ongoing at Tuskegee University using RBS and mass spectroscopic methods, and at JPL with piezoelectric QCM's.

Acknowledgments

This work was supported by the National Aeronautics and Space Administration through a contract with the California Institute of Technology.

The authors wish to express their thanks to Dr. J. Polk (JPL) and E. Boer (Caltech) for critical reading of the manuscript.

References

1. Brophy, J. R., Polk, J. E., and Rawlin, V. K., "Ion Engine Service Life Validation by Analysis and Testing," AIAA 96-2715, presented at the 32nd AIAA/ASME/SAE/ASEE Joint Propulsion Conference, Lake Buena Vista, FL (July 1996).
2. O'Brian, C. D., Lindner, A., Moore, W. J., J. Chem. Phys. **29**, 3 (1958).
3. Kenknight, C. E., and Wehner, G. K., J. Appl. Phys. **35**, 322 (1964).
4. Crasten, J. L., Hancox, R., Robson, A. E., Kaufmann, S., Miles, H. T., Ware, A., and Wessen, J. A., Proc. 2nd Intern. Conf. Atom. Energy **32**, 414 (1958).
5. Wehner, G. K., and Anderson, G. S., "The Nature of Physical Sputtering," *Handbook of Thin Film Technology*, Maissel, L. I., and Glang, R., editors (1970).
6. Behrisch, R., Sigmund, P., Robinson, M. T., Andersen H. H., Bay, H. L. and Roosendaal, H. E., *Sputtering by Particle Bombardment I: Physical Sputtering of Single-Element Solids*, Topics in Applied Physics **47**, Springer-Verlag (1981).
7. Behrisch, R., Maderlechner, G., Scherzer, B. M. U., and Robinson, M. T., "The Sputtering Mechanism for Low-Energy Light Ions," J. Appl. Phys. **18**, 391 (1979).
8. Wehner, G. K., and Rosenberg, D., J. Appl. Phys. **31**, 177 (1960).
9. Olson, R. R., King, M. E., and Wehner, G. K., "Mass Effects on Angular Distribution of Sputtered Atoms," J. Appl. Phys. **50** (5), 3677 (1979).
10. Ziegler, J. F., Biersack, J. P., and Littmark, U., *The Stopping and Range of Ions in Solids*, Ziegler, J. F. editor (1985).
11. Weissmann, R., and Sigmund, P., "Sputtering and Backscattering of keV Light Ions Bombarding Random Targets," Radiation Effects **19**, 7-14 (1973).

12. Wehner, G. K., "Low-Energy Sputtering Yields in Hg," Physical Review **112** (4), 1120 (1958).
13. Bradley, R., C., "Sputtering of Alkali Atoms by Inert Gas Ions of Low Energy," Physical Review **93** (4), 719 (1954).
14. Stuart, R. V., and Wehner, G. K., "Sputtering Yields at Very Low Bombarding Ion Energies," J. of Appl. Phys. **33** (7), 2345 (1962).
15. Askerov, S. G., and Sena, L. A., "Cathode Sputtering of Metals by Slow Mercury Ions," Soviet Phys. - Solid State **11** (6), 1288 (1969).
16. Bay, H. L., Roth, J., and Bohdansky, J., "Light-Ions Sputtering Yields For Molybdenum and Gold at Low Energies," J. of Appl. Phys. **48** (11), 4722 (1977).
17. Bohdansky, J., Roth, J., and Bay, H. L., "An Analytical Formula and Important Parameters for Low-Energy Ion Sputtering," J. of Appl. Phys. **51** (5), 2861 (1980).
18. Yamamura, Y., Matsunami, N., and Itoh, N., Radiat. Eff. Lett. **68**, 83 (1982).
19. Yamamura, Y., Matsunami, N., and Itoh, N., Radiat. Eff. Lett. **71**, 65 (1983).
20. Weissmann, R., and Behrisch, R., Radiat. Eff. **19**, 69 (1973).
21. Yamamura, Y., Itikawa, Y., and Itoh, N., "Angular Dependence of Sputtering Yields of Monoatomic Solids," Report IPPJ-AM-26, Institute of Plasma Physics, Nagoya University, Japan (1983).
22. Sigmund, P., "Theory of Sputtering. I. Sputtering Yield of Amorphous and Polycristalline Targets," Phys. Rev. **184** (2), 383 (1969).
23. Lindhard, J., Scharff, M., and Schiott, H. E., Mat. Fys. Medd. Dan. Vid. Selsk. **33**, 14 (1963).
24. Rawlin, V. K., "Screen Grid Wear at Low Flow and High Beam Current Conditions," NSTAR Memorandum, Lewis Research Center Document (April 1996).
25. Matsunami, N., Yamamura, Y., Itikawa, Y., Itoh, N., Kazumata, Y., Miyagawa, S., Morita, K., and Shimizu, R., "A Semi-empirical Formula for the Energy Dependence of the Sputtering Yield," Rad. Eff. Lett. **57**, 15 (1980).
26. Yamamura, Y., Matsunami, N., and Itoh, N., "A New Empirical Formula for the Sputtering Yield," Rad. Eff. Lett. **68**, 83 (1982).
27. Yamamura, Y., Matsunami, N., and Itoh, N., "Theoretical Studies on an Empirical Formula for Sputtering Yield at Normal Incidence," Radiat. Eff. **71**, 65 (1983).
28. Matsunami, N., Yamamura, Y., Itikawa, Y., Itoh, N., Kazumata, Y., Miyagawa, S., Morita, K., Shimizu, R., and Tawara, H., "Energy Dependence of the Ion-Induced Sputtering Yields of Monoatomic Solids," Atomic Data and Nuclear Data Tables **31**, 1 (1984).
29. Bohdansky, J., "A Universal Relation for the Sputtering Yield of Monoatomic Solids at Normal Ion Incidence," Nucl. Instr. and Meth. in Phys. Res. **B2**, 587 (1984).
30. Bond, R., and Latham, M., "Ion Thruster Extraction Grid Design and Erosion Modelling using Computer Simulation," AIAA 95-2923, presented at the 31st AIAA/ASME/SAE/ASEE Joint Propulsion Conference, San Diego, CA (July 1995).
31. Blandino, J. J., Goodwin, D. G., and Garner, C. E., "Evaluation of Diamond Grids for Ion Thruster Optics: Low Energy Sputter Yield Measurements," AIAA 96-3203, presented at the 32nd AIAA/ASME/SAE/ASEE Joint Propulsion Conference, Lake Buena Vista, FL (July 1996).
32. Bhattacharjee, S., Zhang, J., Shutthanandan, V., Ray, P. K., Shivaparan, N. R., Smith, R. J., "Application of Secondary Neutral Mass Spectrometry in Low-Energy Sputtering Yield Measurements," Nucl. Instr. and Meth. in Phys. Res. **B129**, 123 (1997).
33. Rosenberg, D., and Wehner, G. K., "Sputtering Yields for Low Energy He^+-, Kr^+-, and Xe^+-Ion Bombardment," J. of Appl. Phys. **33** (5), 1842 (1962).
34. Weijsenfeld, C. H., Hoogendoorn, A., and Koedam, M., "Sputtering of Polycrystalline Metals by Inert Gas Ions of Low Energy (100-1000 eV)," Physica **27**, 763 (1961).
35. Wehner, G. K., "Sputtering Yields for Normally Incident Hg^+-Ion Bombardment at Low Ion Energy," Phys. Rev. **108** (1), 35 (1957).
36. Rawlin, V. K., and Mantenieks, M. A., "Effect of Facility Background Gases on Internal Erosion of the 30-cm Hg Ion Thruster, " AIAA paper 78-665 (1978).
37. Mantenieks, M. A., and Rawlin, V. K., "Sputtering in Mercury Ion Thrusters," *Electric Propulsion and Its Application to Space Missions* edited by Robert C. Finke, Progress in Astronautics and Aeronautics **79**, (1981).
38. Abe, T., and Yamashina, T., " The Deposition Rate of Metallic Thin Films in the Reactive Sputtering Process," Thin Solid Films **30**, 19 (1975).
39. Behrisch, R., *Festkörperzerstäubung durch Ionen-beschuß*, Ergeb. Exakten Naturwiss **35**, 295 (1964).
40. Winters, H. F., and Sigmund, P., "Sputtering of Chemisorbed Gas (Nitrogen and Tungsten) by Low Energy Ions," J. Appl. Phys. **45**, 4760 (1974).
41. Winters, H. F., and Taglauer, E., "Sputtering of Chemisorbed Nitrogen from Single-Crystal Planes of Tungsten and Molybdenum," Phys. Rev. **B35**, 2174 (1987).
42. Beattie, J. R., " A Model for Predicting the Wearout Lifetime of the LeRC/Hughes 30-cm Mercury Ion Thruster," AIAA paper 79-2079 (1979).
43. Laegreid, N., and Wehner, G. K., "Sputtering Yileds of Metals for Ar^+ and Ne^+ Ions with Energies from 50 to 600 eV," J. of Appl. Phys. **32** (3), 365 (1961).
44. Behrisch, R., Bohdansky, J., Oetjen, G. H., Roth, J., Schilling, G., and Verbeek, H., "Measurements of the Erosion of Stainless Steel, Carbon, and SiC by Hydrogen Bombardment in the Energy Range of 0.5-7.5 keV," J. of Nuclear Materials **60**, 321 (1976).
45. Hechtl, E., Bay, H. L., and Bohdansky, J., "Low Energy Selfsputtering Yields of Nickel," Appl. Phys. **16**, 147 (1978).
46. Bay, H. L., Bohdansky, J., Hofer, W. O., and Roth, J., "Angular Distribution and Differential Sputtering Yields for Low-Energy Light-Ion Irradiation of Polycrystalline Nickel and Tungsten," Applied Phys. **21**, 327 (1980).
47. Okajima ,Y., "Estimation of Sputtering Rate by Bombardment with Argon Gas Ions," J. Appl. Phys. **51** (1), 715 (1980).
48. Blandino, J. J., Goodwin, D. G., Garner, C. E., and Brophy, J. R., "Evaluation and Development of Diamond Grids for Ion Optics," AIAA 95-2663, presented at the 31st AIAA/ASME/SAE/ASEE Joint Propulsion Conference, San Diego, CA (July 1995).
49. Askerov, S. G., and Sena, L. A., "Cathode Sputtering of Metals by Slow Mercury Ions," Soviet Phys.- Solid State **11** (6), 1288 (1969).
50. Morgulis, N. D., and Tishchenko, V. D., "The Investigation of Cathode Sputtering in the Near Threshold Region. I," Soviet Phys. JETP **3** (1), 52 (1956).
51. Handoo, A. K., Ray, P. K., "Modeling of Life Limiting Phenomena in the Discharge Chamber of an Electron Bombardment Ion Thruster," NASA report NAG 8-020 (1991).
52. Handoo, A. K., Ray, P. K., "Sputtering Yield of Chromium by Argon and Xenon Ions with Energies from 50 to 500 eV," Appl. Phys. **A54**, 92 (1992).
53. Handoo, A. K., Ray, P. K., "Sputtering of Cobalt and Chromium by Argon and Xenon Ions Near the Threshold Energy Region," Can. J. Phys. **71**, 155 (1993).
54. Polk, J. E., "Mechanisms of Cathode Erosion in Plasma Thrusters," Thesis Report, Princeton Univ., NJ. (1996).
55. McKeown, D., "New Method for Measuring Sputtering in the Region near Threshold," The Rev. of Scientific Instruments **32** (2), 133 (1960).
56. Hayward, W. H., and Wolter, A. R., "Sputtering Yield Measurements with Low-Energy Metal Ion Beams," J. of Appl. Phys. **40** (7), 2911 (1968).
57. Stuart, R. V., Wehner, G. K., "Sputtering Thresholds and Displacement Energies," Phys. Rev. Lett. **4** (8), 409 (1960).
58. Rock, B. A., Mantenieks, M. A., and Parsons, M. L., "Rapid Evaluation of Ion Thruster Lifetime Using Optical Emission Spectroscopy," NASA report TM-87103 or AIAA-85-2011 (1985).
59. Smith, J. N. Jr, Meyer, C. H. Jr, and Layton, J. K., "Auger Electron Spectroscopy in Sputtering Measurements: Application to Low-Energy Ar^+ Sputtering of Ag and Nb," J. of Appl. Phys. **46** (10), 4291 (1975).